

Strain-controlled insulator-metal transition in $\text{YTiO}_3/\text{SrTiO}_3$ superlattices: effect of interfacial reconstruction

Xue-Jing Zhang,^{1,2} Peng Chen,^{1,2} and Bang-Gui Liu^{1,2,*}

¹*Beijing National Laboratory for Condensed Matter Physics,
Institute of Physics, Chinese Academy of Sciences, Beijing 100190, China*

²*School of Physical Sciences, University of Chinese Academy of Sciences, Beijing 100190, China*

I. PRELIMINARY STUDY ON BULK SrTiO_3 AND YTiO_3

The optimized lattice constants a of SrTiO_3 (STO) with PBE and PBEsol are 5.61 and 5.55 Å, being larger than experimental lattice constant by 1.6% and 0.5%, respectively. As for YTiO_3 (YTO), PBE and PBEsol produce the lattice constants $a/b/c$: 5.409/5.761/7.772 and 5.340/5.725/7.636 Å.

b , and c are the lattice constants) with PBE and PBEsol for STO are 1, equal to the experimental value. The calculated $(c/a, c/b)$ with PBE and PBEsol for YTO are (1.437, 1.349) and (1.430, 1.334), respectively, being close to the experimental value (1.432, 1.340). The calculated spin-resolved electronic band structures of the STO and YTO with experimental lattice constants for PBE and PBEsol are shown in Fig. S1. It can be seen the band structures with PBE and PBEsol are similar.

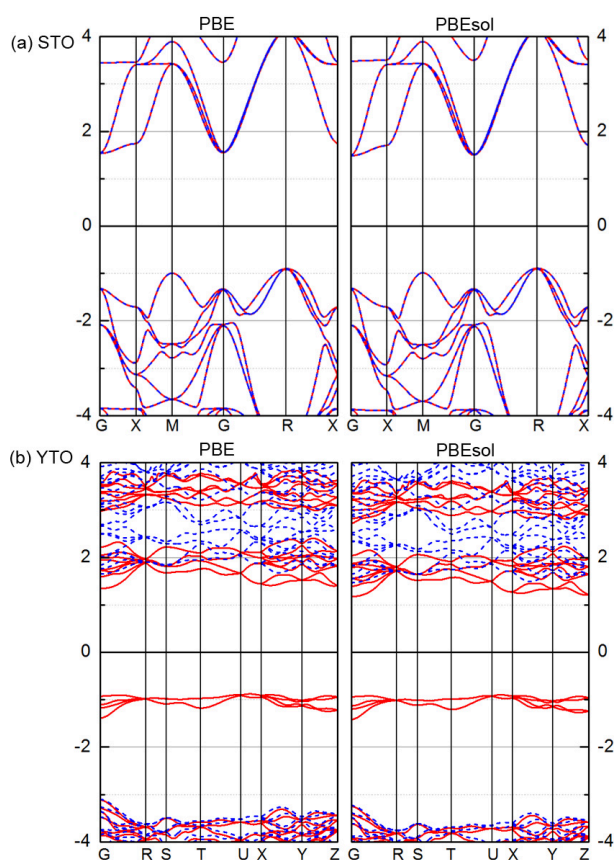


FIG. S1. (Color online) Spin-resolved electronic band structures of the bulk STO (a) and the bulk YTO (b) calculated with PBE and PBEsol. The red and blue lines represent the spin-up and spin-down states, respectively.

The calculated structural parameters c/a and c/b (a ,

II. STRUCTURAL AND ELECTRONIC PROPERTIES OF THE $(\text{STO})_4/(\text{YTO})_2$ SUPERLATTICE

The magnetization density distribution of the $(\text{STO})_4/(\text{YTO})_2$ superlattice for $\epsilon_s=0\%$ and -2% are presented in Fig. S2.

The various Ti-O bond lengths of the TiO_6 octahedra in the $(\text{STO})_4/(\text{YTO})_2$ superlattice for $\epsilon_s=0\%$ and -2% are presented in Fig. S3.

We consider YTO, with space group Pbnm, grown on STO single-crystal substrate. Therefore, the in-plane lattice constant of the superlattice is fixed to the experimental lattice constant of STO ($\sqrt{2}a = 5.52$ Å) for the zero strain, and our calculated results indicate the structural phase transition takes place near -0.2% .

If we replace the experimental value with the PBE optimized value for the in-plane lattice parameter for the zero strain point, the structural phase transition should take place at $\epsilon_s = -1.8\%$. This means that the strain value for the structural phase transition is changed a little when the in-plane lattice constant is changed from the experimental value to the PBE value.

If we replace PBE with PBEsol and the in-plane lattice constant of the superlattice is fixed to the experimental lattice constant of STO ($\sqrt{2}a = 5.52$ Å) for the zero strain, the calculated structural phase transition point takes place near -1.35% , as shown in Fig. S4. This means that if we replace the experimental value of the in-plane lattice parameter for the zero strain point with the PBEsol optimized value, the structural phase transition should take place at $\epsilon_s = -1.85\%$ because the PBEsol optimized lattice constant of STO is larger than experimental one by 0.5%.

* bgliu@iphy.ac.cn

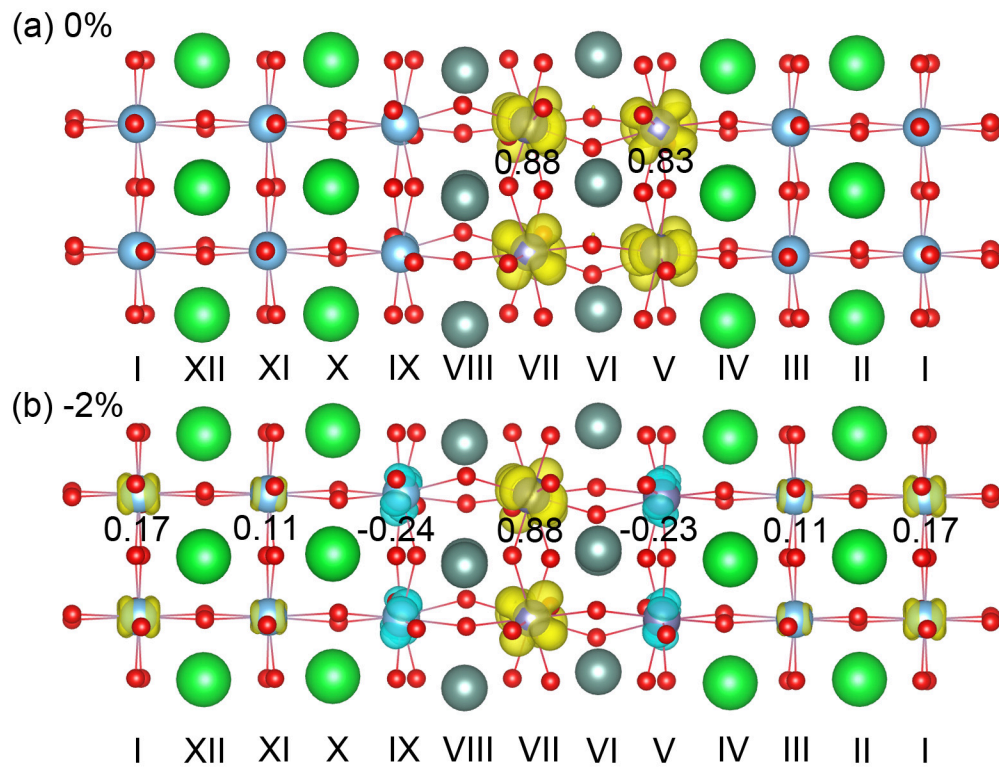


FIG. S2. (Color online) Two magnetization-density isosurfaces of the $(\text{STO})_4/(\text{YTO})_2$ superlattice at $\epsilon_s=0\%$ (a) and -2% (b). The yellow and cyan isosurfaces correspond to $+0.006\mu_B/\text{\AA}^3$ and $-0.006\mu_B/\text{\AA}^3$, respectively.

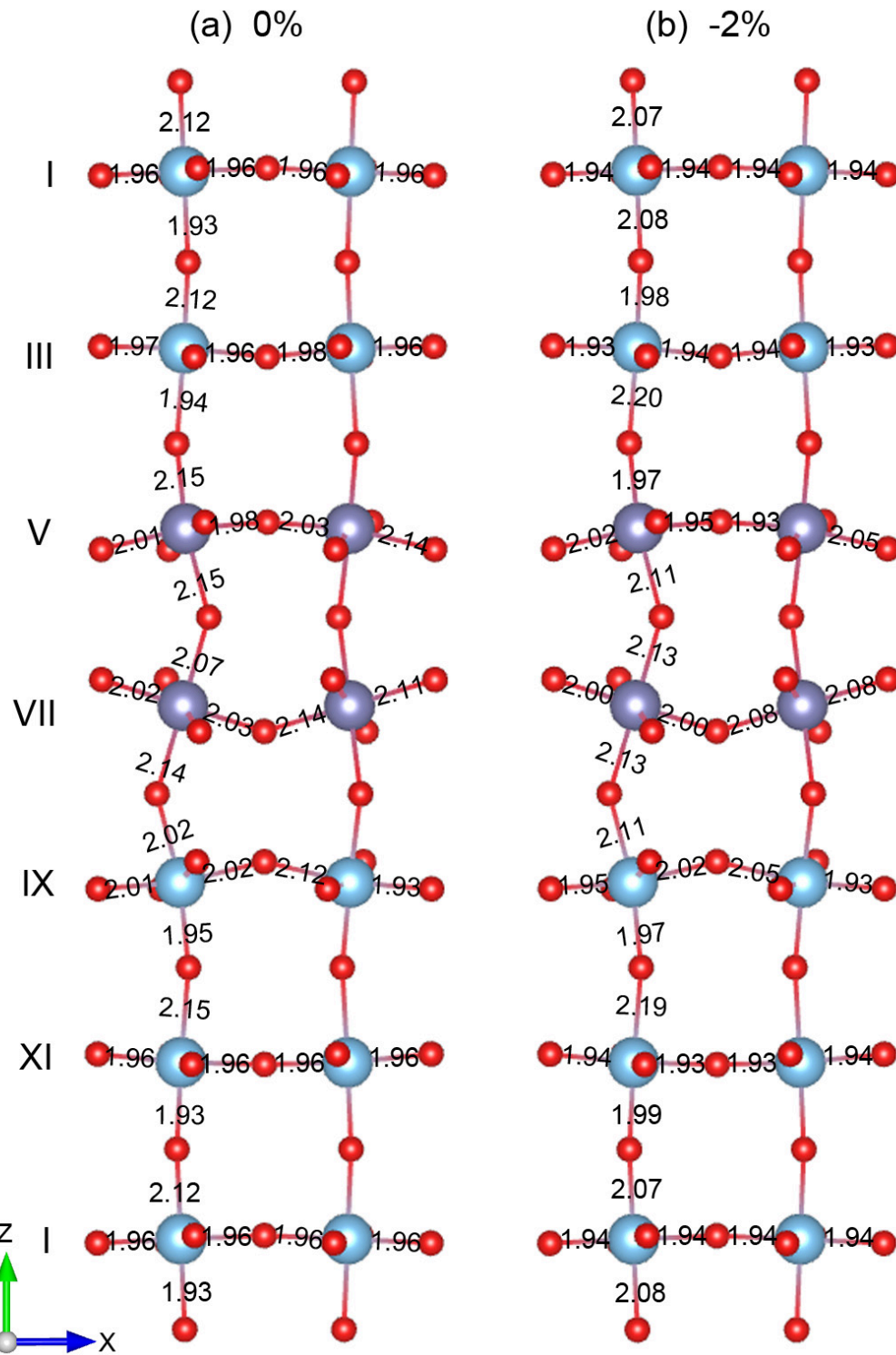


FIG. S3. (Color online) The various Ti-O bond lengths of the TiO_6 octahedra in the $(\text{STO})_4/(\text{YTO})_2$ superlattice at $\epsilon_s=0\%$ (a) and -2% (b), respectively.

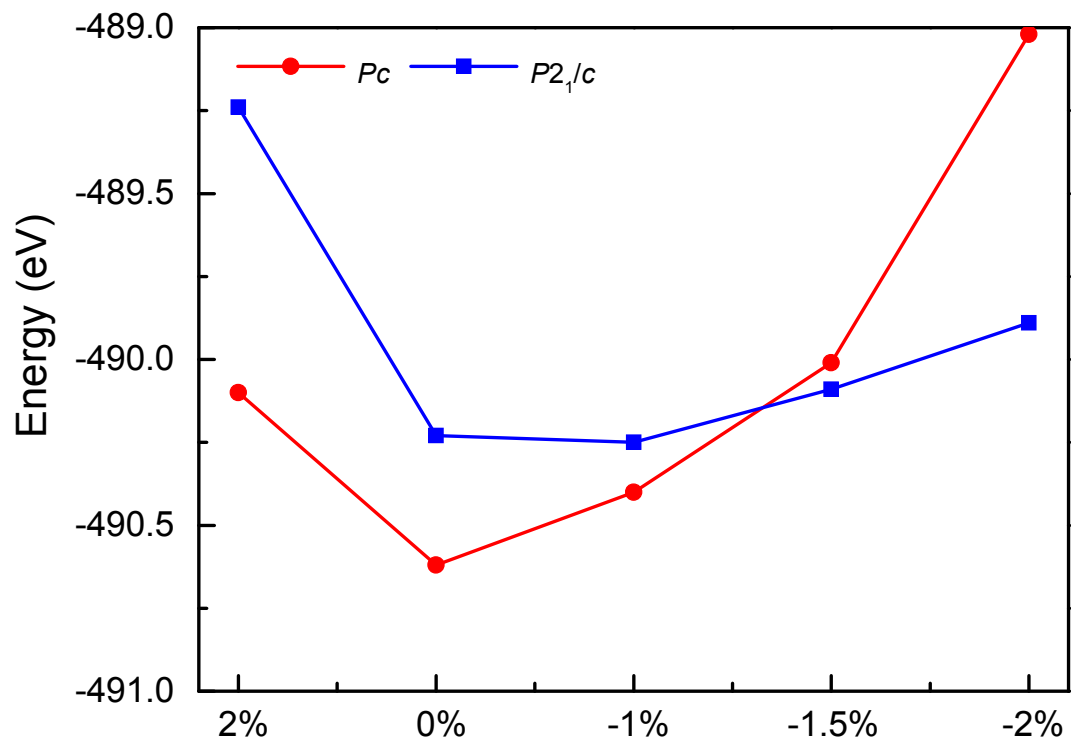


FIG. S4. (Color online) A comparison of PBEsol total energies of the P_a (red, Pc) and P_b (blue, $P2_1/c$) structures with the strain changing from $\varepsilon_s = 2\%$ to -2% .